Nanoscale

Accepted Manuscript

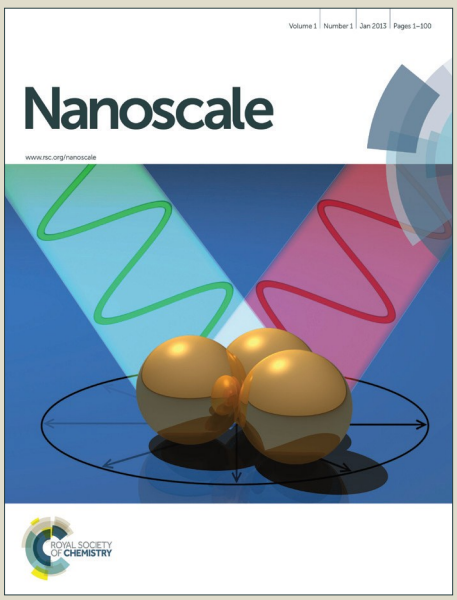

ROYAL SOCIETY OF CHEMISTRY

www.rsc.org/nanoscale

Journal Name

ARTICLE

Highly sensitive self-complementary DNA nanoswitches triggered by polyeletrolytes

Received 00th January 20xx,
Accepted 00th January 20xx

DOI: 10.1039/x0xx00000x

www.rsc.org/

Jincai Wu,[a§] Feng Yu,[a§] Zheng Zhang,[a] Yong Chen,[a] Jie Du,*[a] and Atsushi Maruyama*[b]

Dimerization of two homologous strands of genomic DNA/RNA is an essential feature of retroviral replication. Herein we show that a cationic comb-type copolymer (CCC), poly(L-lysine)-*graft*-dextran, accelerates dimerization of self-complementary stem-loop DNA, frequently found in functional DNA/RNA molecules, such as aptamers. Further, an anionic polymer poly(sodium vinylsulfonate) (PVS) dissociates CCC from the duplex shortly within a few seconds. Then single stem-loop DNA spontaneously transforms from its dimer. Thus we can easily control the dimer and stem-loop DNA by switching on/off CCC activity. Both polyelectrolytes and DNA concentrations are nanomole per liter range. The polyelectrolytes-assisted transconformation and sequences design strategy insures the reversible states control with rapid response and effective switching under physiologically relevant conditions. A further application of this sensitive assembly is to construct an aptamer-type drug delivery system, bind or release functional molecules responding to its transconformation.

Introduction

Nanometer-scaled DNA devices based on programmed assembly of DNA helices has become a powerful tool in DNA nanotechnology fields beyond its biological importance.[1-4] Numerous endeavors have been reported on the use of light irradiation[5-8], changes in environmental pH[9-14]or ion[15,16], and the addition of DNA oligonucleotides[17-20] or enzymes[21-23] as external stimuli for DNA nanomachines.

For most of DNA nanomachines constructed so far, oligonucleotides have been generally used as fuels. The common operating principles employed in this DNA-fueled nanomachine involve sequence-specific hybridizations and strand exchange reactions between the machine body and the sequential addition of DNA fuels. However, the operation conditions of the DNA-fueled nanomachines are limited. For example, the switch frequency is limited by the hybridization kinetics of complementary strands; it needs for high concentration of DNA oligonucleotide to retain the machine's dynamic action; a DNA duplex waste is produced in each cycle, accumulation of the waste products leads to a progressive loss of operating efficiency.[24,25] To overcome these weaknesses, a new strategy is therefore required for the development of DNA nanotechnology.

Our group developed a cationic copolymer-assisted strategy to solve this problem using G-quadruplex and DNA tweezer nanomachines as models.[26,27] This strategy is partially an extended work of our previous studies on interactions between cationic comb-type copolymers (CCCs) and triplex or duplex DNA. [28-30] In those studies, we demonstrated that CCCs composed of a polycation backbone and abundant hydrophilic graft chains (> 90 wt%) influence kinetics and thermodynamics of nucleic acid hybridization under physiologically relevant conditions. Detailedly, we found the Poly(L-lysine)-*graft*-dextran (PLL-*g*-Dex) copolymer significantly accelerates DNA hybridization.[31] Moreover, the copolymer markedly accelerates the strand-exchange reaction (SER) and increases the stability of dsDNA relative to that in buffer alone.[32-34] The SER acceleration of the copolymer has been applied for refining the DNA detection method[35-37] and DNA nanodevices with improved response even at 200 times lower strand concentration (nanomole per liter range) than those in other report.[20,27] The foundation of our researches is the interaction mechanism of CCCs and nucleic acid. The CCCs reduce an entropically unfavourable counterion condensation effect that accompanies a nucleation process of SER, lowering the energy barrier associated with breakage and reassociation of nucleic acid base pairs. [32]

Nucleic acid chaperones catalyze the folding of nucleic acid into the most stable conformation. As artificial nucleic acid chaperones, a unique aspect of CCCs is that they accelerate the SER while stabilizing DNA hybrids. A naturally occurring nucleic acid chaperone, HIV-1 NCp7, also have the nucleic acid chaperone activity and play a crucial role in proviral life cycle.[38,39] Dimerization of two homologous strands of genomic RNA is an essential feature of retroviral replication. In HIV-1, a conserved stem-loop sequence, the dimerization initiation site (DIS), has been identified as the domain primarily responsible

[a] College of Materials and Chemistry Engineering, Hainan University, Haikou 570228, China. E-mail: dujie@hainu.edu.cn
[b] Department of Biomolecular Engineering, Graduate School of Bioscience and Biotechnology, Tokyo Institute of Technology, 4259-B57 Nagatsuta, Midori, Yokohama, 226-8501, Japan. E-mail: amaruyama@bio.titech.ac.jp
§ J. C. W. and F. Y. contributed equally to this paper.
† Electronic Supplementary Information (ESI) available. See
DOI: 10.1039/x0xx00000x

for initiation of this aspect of viral assembly.[40,41] The DIS loop contains a self-complementary sequence and can form a homodimer through a loop-loop kissing interaction. NCp7 acts catalytically to induce the structural isomerization by accelerating strand exchange between the two stem-loops, converts DIS dimer to an extended duplex isoform.

Herein we examined the activity of CCCs to trigger the dimerization of a self-complementary stem-loop DNA, DIS25, similar as DIS in HIV-1 genome. The purpose of this study was to test whether CCCs facilitate dimerization of DIS like as NCp7. Further, we assessed whether the anionic polymer could switch off CCCs activity, soon dissociating single stem-loop DIS from its dimer. If this strategy is viable, we can easily control DIS dimer and single stem-loop by switching on/off CCCs activity. A biomedical application of this programmable assembly is to construct a smart aptamer-type nanoswitch that can bind or release functional molecules responding to its transconformation. Beyond this objective, the reversible state control with rapid response and effective switching is in great need, which is the main work in this paper.

Experimental

Materials: All oligonucleotides were supplied by FASMAC Co., Ltd. and purified by reverse-phase high performance liquid chromatography. The sequence of DIS25, DIS25-2a, DIS25-3a; T_m of stem-loop DNA and dimer were detailed listed in **Fig. S1** (ESI‡). Cationic comb-type copolymer PLL-*g*-Dex (M_n = 65,000) was prepared by a reductive amination reaction of PLL·HBr (M_n = 20,000, BACHEM) with dextran (M_n = 5,900, Dextran T-10, Amersham Pharmacia Biotech) as described previously.[28] The dextran content of the copolymer was 91 wt% as determined by ^{1}H NMR (**Fig. S2**, ESI‡). DNA samples were treated by annealing (heating to 90 ^{o}C for 5 min and quick cooling on ice). PLL-*g*-Dex/DNA complex was constructed at various N/P ratios (the ratios of moles of the amine groups of cationic polymers to those of the phosphate ones of DNA).

Native polyacrylamide gel electrophoresis: DNA solutions were prepared in 10 mM sodium phosphate buffer (pH 7.2) containing 0.5 mM EDTA and 150 mM NaCl with or without PLL-g-Dex. DNA samples were incubated at 37 ^{o}C for 1 h or 3 h. Native PAGE (13%) was performed in TBE buffer at 25 ^{o}C for 2 h at 100 V. After electrophoresis, the gel was stained with 0.01 % EtBr.

Fluorescence spectroscopy: The DNA solution (4:1 mixture of non-labeled DIS25 and TAMRA and DABCYL double-labeled DIS25, T-DIS25-D) was dissolved in sodium phosphate buffer (10 mM sodium phosphate, 0.5 mM EDTA, 150 mM NaCl, pH 7.2). Baseline emission values were first recorded for about 5 minutes, and then PLL-g-Dex and PVS were successively added to the DNA solution with a syringe. The change in fluorescence intensity of the mixture (total volume 2 ml) in a 10 mm-square quartz cuvette was recorded on a JASCO FP-6500 fluorescence spectrometer (JASCO) with a Peltier thermostatically controlled cell holder at excitation and emission wavelengths of 540 nm and 570 nm, respectively. The TAMRA emission of T-DIS25-D is quenched by DABCYL when T-DIS25-D folds into the stem-loop structure. The TAMRA emission recovers when T-DIS25-D forms a dimer with non-labeled DIS25.

UV-melting point (T_m) measurement: Final DNA concentration of 2 μM (DIS25) in sodium phosphate buffer (10 mM sodium phosphate, 0.5 mM EDTA, 150 mM NaCl, pH 7.2). The mixture of DNA solution was heated at 95 ^{o}C for 3 min and gradually cooled to r.t. UV spectra at 260 nm was recorded by a Shimadzu UV-1650 PC spectrometer equipped with a TMSPC-8 temperature controller (Shimadzu, Kyoto, Japan). Melting curves were obtained at a heating rate of 0.5 ^{o}C/min and a cooling rate of 0.5 ^{o}C/min.

Results and discussion

Firstly, the effect of CCC, PLL-*g*-Dex on DIS25 dimerization was evaluated by native polyacrylamide gel electrophoresis (PAGE) assay using a 4:1 mixture of non-labeled DIS25 and TAMRA and DABCYL double-labeled DIS25, T-DIS25-D. DIS25 and T-DIS25-D mixture (2 μM) were incubated at 25 °C in 10 mM sodium phosphate buffer (pH 7.2) containing 150 mM NaCl and 0.5 mM EDTA in the absence or presence of PLL-g-Dex (N/P = 1) for 1 h or 3 h.

After the incubation, 0.2wt% poly(sodium vinylsulfonate) (PVS) was added to dissociate each copolymer from DNA. Gel electrophoresis was then carried out on a 13% polyacrylamide gel at 4 °C in TBE buffer. The TAMRA emission of T-DIS25-D is quenched by DABCYL when T-DIS25-D folds into the stem-loop structure. The TAMRA emission recovers when T-DIS25-D forms a dimer with non-labeled DIS25. **Fig. 1A** shows PAGE images acquired by TAMRA emission or EtBr staining. The band with higher electrophoretic mobility is identified as the stem-loop monomer. After the gel is stained with EtBr, the both monomer and dimer bands can be captured. The gel images showed that the dimerization of DIS25/T-DIS25-D in the absence of PLL-*g*-Dex hardly occurred even after 3 h incubation. On the other hand, the hybridization was accelerated by PLL-*g*-Dex, which revealed that PLL-*g*-Dex thermodynamically stabilizes the intermolecular dimer preferentially over the stem-loop intramolecular structure. Another study with more PLL-*g*-Dex (N/P=2, N/P=6) and longer incubation (3h, 10h, 24h) evaluated by PAGE was shown in **Fig. S3** (ESI‡). The results further testified that PLL-*g*-Dex markedly facilitates dimer formation. Note that upper bands of DNA in the presence of PLL-*g*-Dex are in the same level with the band of DNA after renaturation process (heating to 90 ^{o}C for 5 min and slowly cooling to room temperature), which confirms that the upper band is for DNA duplex, not for coil single strand with two ends far away from each other.

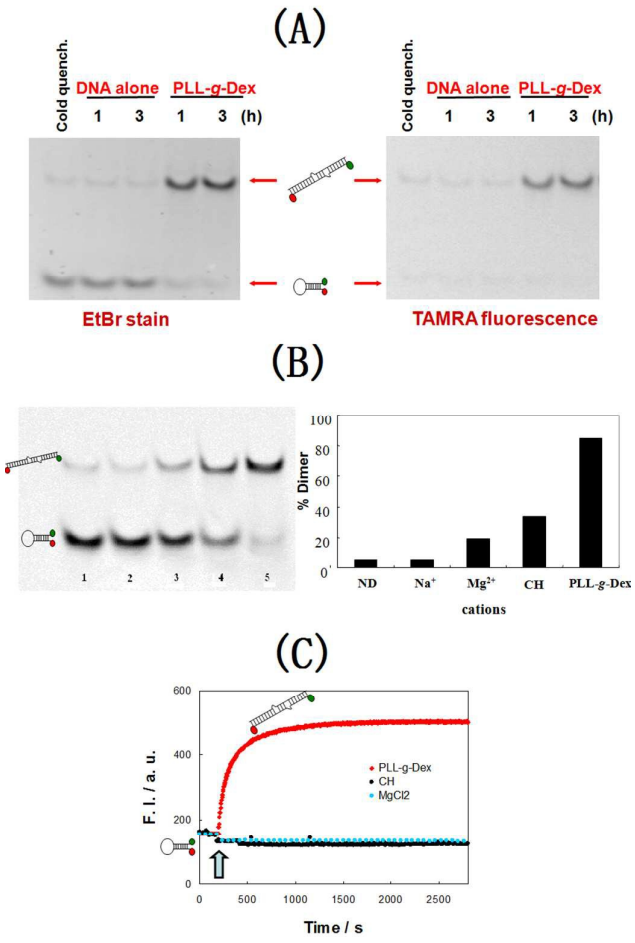

Fig. 1 (A) Gel electrophoretic analysis of dimerization of DIS25 with or without PLL-*g*-Dex. [DIS25] =1.6 μM, [T-DIS25-D] = 0.4 μM, N/P = 1. (B) Gel electrophoretic analysis of dependency of dimerization of DIS25 on the cationic substance. [DIS25] =1.6 μM, [T-DIS25-D] = 0.4 μM, in 10 mM sodium phosphate buffer (pH 7.2, 0.5 mM EDTA, 150 mM NaCl), 37 °C for 2 h. Lane 1, no additive (quench); lane 2, no additive; lane 3, 5 mM $MgCl_2$; lane 4, 500 μM $[Co(NH_3)_6]^{3+}$; lane 5, 100 μM PLL-*g*-Dex. The gel image was captured with EtBr staining. (C) Time course of dimerization of DIS25 in the presence of different cationic substances. A stirred DNA solution ([DIS25] =80 nM, [T-DIS25-D] = 20 nM) in 10 mM sodium phosphate buffer (pH 7.2, 0.5 mM EDTA, 150 mM NaCl) was mixed at 37 °C with 5 mM Mg^{2+} (cyan), 500 μM $[Co(NH_3)_6]^{3+}$ (black), and 100 μM PLL-*g*-Dex (red).

We then compared the activity of the copolymer (100 μM PLL-*g*-Dex) to those of different cationic substances, 5 mM Mg^{2+} and 500 μM $[Co(NH_3)_6]^{3+}$ under physiologically relevant conditions, pH 7.2, containing 150 mM NaCl at 37 °C. As shown in **Fig. 1B**, 5 mM Mg^{2+} and 500 μM $[Co(NH_3)_6]^{3+}$ resulted in 18% and 42%, respectively, conversion to DIS25 dimer, while PLL-*g*-Dex at lower concentration (100 μM) induced almost full conversion (>90%) to the dimer state from the stem-loop state. The result implied an effective stablilization effect of CCC on DIS25 dimer.

In order to observe kinetic effect of the cationic substances on the dimerization reaction in real time with a resolution of seconds, we employed fluorescence resonance energy transfer (FRET) assay. **Fig. 1C** showed that when we added PLL-g-Dex into the DNA solution, the fluorescence intensity increased to the maximum value within 900 s. The fluorescence intensity changes were not obvious in other cationic substances. These results showed that PLL-g-Dex significantly accelerated dimerization to stabilize the linear dimer structure even at 100 nM DNA concentration.

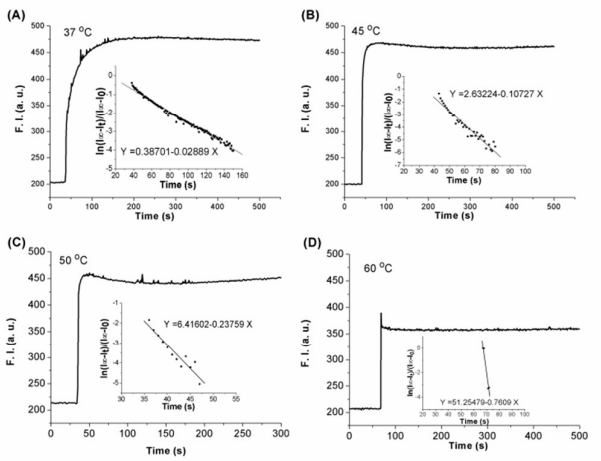

Fig. 2 Kinetic dimerization of DIS25 triggered by PLL-*g*-Dex (*N/P*=1). A stirred DNA solution ([DIS25] =90 nM, [T-DIS25-D] = 10 nM) in 10 mM sodium phosphate buffer (pH 7.2, 0.5 mM EDTA, 150 mM NaCl) was mixed (A) at 37 °C, (B) at 45 °C, (C) at 50 °C, (D) at 60 °C. The value of fluorescence intensity was calculated with the following equation to yield a rate constant of the second-order reaction. $kt = ln[(I_\infty - I_t)/(I_\infty - I_0)]$. Where I_0 is the initial fluorescence intensity of TAMRA-labeled DNA, I_t is that at time *t*, and I_∞ is that after the reaction reached equilibrium.

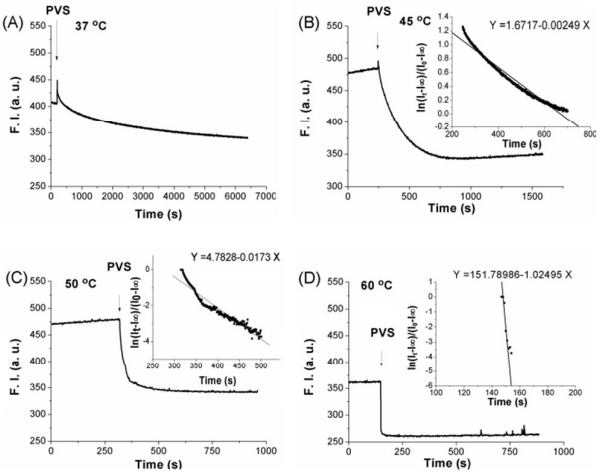

Fig. 3 Kinetic dissociation of DIS25 dimer triggered by PVS (1.2 times excess added after the course in Fig. 3). (A) at 37 °C, (B) at 45 °C, (C) at 50 °C, (D) at 60 °C. The value of fluorescence intensity was calculated with the following equation to yield a rate constant of the second-order reaction. $kt = ln[(I_t - I_\infty)/(I_0 - I_\infty)]$. Where I_0 is the initial fluorescence intensity of TAMRA-labeled DNA before adding PVS, I_t is that at time *t*, and I_∞ is that after the reaction reached equilibrium.

During the dimerization formation, CCCs spontaneously interact with DNA to form inter-polyelectrolyte complexes. The fluorescence polarization can be used to measure the apparent volume (or molecular weight) of DNA duplex. This measurement is possible because larger duplex rotates more slowly. Hence, if CCC binds to DNA duplex, the rotational rate decreases, and the polarity increases. According to this theory, the fluorescence polarity of DIS25 dimer should be increased after CCC-DNA complex formation. Thus, we can investigate the changes of fluorescence polarity of DNA duplex to examine CCCs' binding. As shown in **Fig. S4** (ESI‡), the fluorescence polarity increased after PLL-*g*-Dex (N/P = 1) added into the DNA solution. To confirm that the increase in the polarity was due to CCC-DNA complex formation, we subsequently added 1.2 times charge concentration an anionic polymer, PVS, to the mixture, and the fluorescence polarity recovered, which shows that the anionic polymer can dissociate the cationic copolymer from the duplex. That means CCCs activity can be switched off by polyanion. Without CCCs chaperoning, could the dimer stably maintain the conformation? To answer this question, the transconformation between the single stem-loop DIS25 and extended dimer induced by switching on/off CCCs activity was evaluated by FRET assay. The kinetic effects of PLL-*g*-Dex/PVS on dimerization of DIS25 or dissociation of dimer at different temperature were also investigated (**Fig. 2, Fig. 3**).

After addition of PLL-*g*-Dex, fluorescence intensity increased, indicating transformation of the stem-loop to the extended dimer form. As shown in **Fig.** 2, with increasing temperature, the dimerization rate was slightly accelerated, while the variation range of the fluorescence intensity decreased above 50 ^{o}C. Note that the dimer was formed even at 60 ^{o}C in presence of PLL-*g*-Dex. The copolymer increased T_m of the dimer from 54.5 ^{o}C (estimated by mFold) to 66.7 ^{o}C as evaluated by UV-T_m analysis (**Fig. S5**, ESI‡).

Subsequent addition of PVS resulted in a relatively slow decrease in the fluorescence intensity, especially at 37 ^{o}C, as shown in **Fig. 3**. Since PVS-induced dissociation of DNA from CCC occurred shortly within a few seconds both at 37 ^{o}C and 60 ^{o}C (**Fig. S4**, ESI‡), indicating PVS easily divests PLL-*g*-Dex–DNA complex of CCCs chaperoning even at a low temperature. Thus the slow decrease in fluorescence intensity (**Fig. 3**) indicated that without CCCs chaperoning the dimer was not still stable and spontaneously transformed to the stem-loop DNA. Further, the spontaneous dissociation of the extended dimer to the stem-loop DNA was considerably slower than the CCC-assisted dimerization. Since the stem-loop (T_m = 62.0 ^{o}C estimated by mFold) is thermodynamically more stable than the extended dimer (T_m = 54.5 ^{o}C estimated by mFold) in the absence of the CCC, transconformation from the dimer to the stem-loop is kinetically restricted by the high energy barrier between dissociation and reassociation of base pairs. As expected, the dissociation rate was accelerated at higher temperature close to T_m. Above 50 ^{o}C, the transition was very rapid (**Fig. 3**). The *E*a value estimated for spontaneous dimer dissociation was 366.2 kJ mol^{-1}, while *E*a of CCC-assisted dimerization was estimated to be 113.2 kJ mol^{-1} (**Fig. S6**, ESI‡), also testified that spontaneous dissociation of the extended dimer to the stem-loop DNA was considerably slower than the CCC-assisted dimerization.

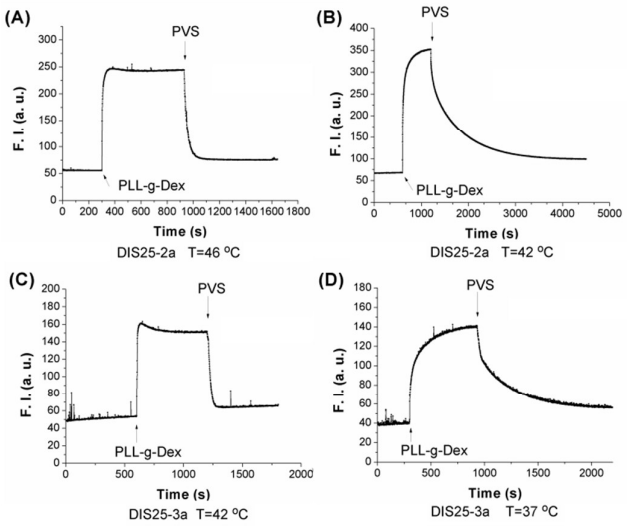

Fig. 4 Dimerization of stem-loop DNA and its dissociation triggered by PLL-*g*-Dex (*N/P*=1) and PVS (1.2 times charge excess). Final concentration of DNA was 50 nM. FRET assay was performed at indicated temperatures in 10 mM sodium phosphate buffer (pH 7.2, 0.5 mM EDTA, 150 mM NaCl). (A) DIS25-2a at 46 ^{o}C. (B) DIS25-2a at 42 ^{o}C. (C) DIS25-3a at 42 ^{o}C. (D) DIS25-3a at 37 ^{o}C.

As mentioned above, at a relatively low temperature such as 37 ^{o}C, the slower dissociation rate resulted in a weaker transconformation response (**Fig. 3**), although the dimerization occurred rapidly in presence of CCC, which provides obstacles to its further application in biological fields. To overcome this limitation, we found that modification of DNA oligonucleotide sequence was a pathway to accelerate the transformation from dimer to stem-loop DNA. We slightly changed the loop sequence of DIS25, changed G/C to A/T. The diverse stem-loop DNA were marked as DIS25-2a and DIS25-3a and the sequences were listed in **Fig. S1** (ESI‡). Estimated by mFold at 2 μM and 150 mM NaCl, the melting temperature of stem-loop DIS25, DIS25-2a and DIS25-3a are same (62.0 ^{o}C), while the melting temperature of dimer DIS25-2a (45.3 ^{o}C) and dimer DIS25-3a (42.3 ^{o}C), lower than dimer DIS25 (54.5 ^{o}C). That means the stabilities of dimer DIS25-2a and DIS25-3a are decreased compared with DIS25, while the stabilities of stem-loop are maintained. In response to the added polyelectrolyte, the transitions of DIS25-2a and DIS25-3a were rapid and reversible and occurred at lower temperatures, 46 ^{o}C and 42 ^{o}C, respectively, as shown in **Fig. 4**.

On the basis of the results above, we can construct a kind of DNA mechanical device that allows easy state control of the reversible extended dimer and single stem-loop DNA by switching on/off CCCs activity. The operating principle employed in this system was shown in **Fig. 5**. This switch can be operated at very low concentration of both DNA and fuels owing to strong interaction between polycation and polyanion or DNA.

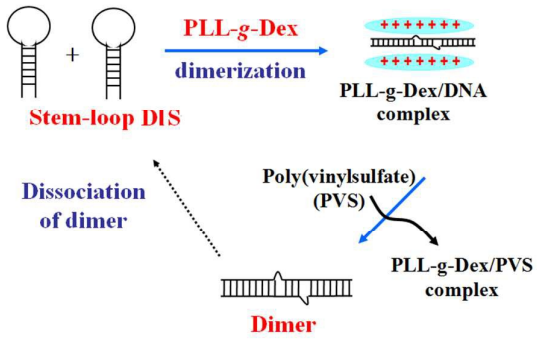

Fig. 5 Switching between stem-loop DNA and extended dimer drived by PLL-g-Dex and PVS.

We carried out FRET assay for the real-time observation the transformations of the nanoswitches. Operating temperature was raised to near T_m of the dimer to obtain quick responses. On this principle, self-complementary DNA nanoswitches (DIS25, DIS25-2a, DIS25-3a series) with high sensitivity driven by polyelectrolyte were constructed respectively at 60 °C, 46 °C and 42 °C, as shown in **Fig. 6A, Fig. 6C,** and **Fig. 6D**. PLL-g-Dex and PVS was added successively, which induced the transformation between dimer and stem-loop DNA. The gel electrophoresis assay testified DIS25 nanoswitch's transformation of the first two cycles in **Fig. 6B**.

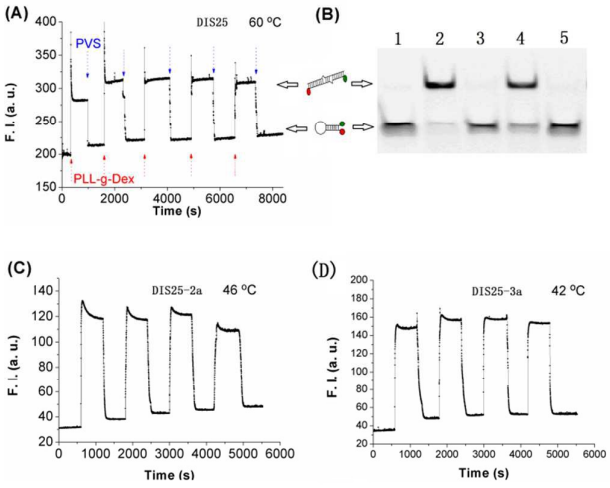

Fig. 6 Transconformation switching of DIS derivatives triggered by polyelectrolytes. Final concentration of DNA was 50 nM. FRET assay was performed at indicated temperatures in 10 mM sodium phosphate buffer (pH 7.2, 0.5 mM EDTA, 150 mM NaCl). PLL-*g*-Dex and PVS (1.2 times excess) were added successively. (A) [DIS25]:[T-DIS25-D] = 4:1, at 60 °C. (B) [DIS25-2a]:[T-DIS25-2a-D] = 39:1, at 46 °C. (C) [DIS25-3a]:[T-DIS25-3a-D] = 39:1, at 42 °C. (D) Gel electrophoretic analysis to confirm transconformation between dimer and single stem-loop DIS25 in response to successive addition of PLL-g-Dex and PVS. Gel images were captured with EtBr staining. Lane 1: DNA alone, Lane 2: 1st PLL- g-Dex addition, Lane 3: 1st PVS addition, Lane 4: 2nd PLL-g-Dex addition, Lane 5: 2nd PVS addition.

Unlike many other DNA-fueled nanomachines, it can operate without a supply of additional DNA strands, and there is no DNA duplex waste produced in each cycle. Therefore, at very low concentration of both DNA and polymer fuels, switching should be highly reversible with negligible change in efficiency. To testify this hypothesis, we changed N/P value in DIS25-3a nanoswitch system at 42 °C (**Fig. 7**). The switching efficiency (N/P=2, **Fig. 7A**) was decreased almost a half in the second cycle. N/P=1.2 (**Fig. 7B**), N/P=1 (**Fig. 7C**) also showed an obvious decrease in switching efficiency after 4 and 6 cycles, respectively. When N/P value was reduced to 0.5, the switching retained well reversible and only slightly decreased in efficiency even after 13 cycles (**Fig. 7E**). Since polycation-polyanion complex produces in each operating cycle, high concentration of this waste polyelectrolyte complex induces loss of switching efficiency after several cycles. Therefore, switching efficiency was increased with N/P value decreasing. Using this programmable strategy, we further designed a double stem-loop DNA (DIS42), and constructed a more complicated nanoswitch system at 37 °C (**Fig. S7**).

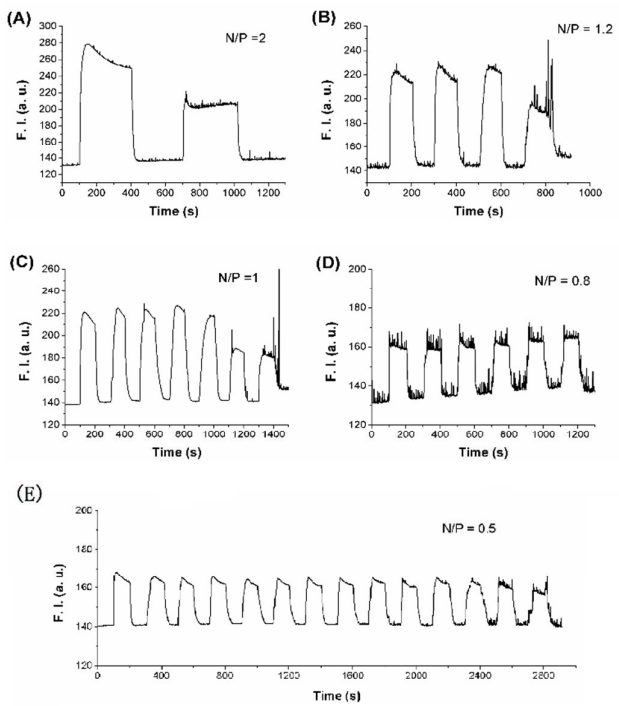

Fig. 7 Transconformation switching of DIS25-3a triggered by polyelectrolytes. Final concentration of DNA was 100 nM ([DIS25-3a]:[T-DIS25-3a-D] = 4:1). FRET assay was performed at indicated temperatures in 10 mM sodium phosphate buffer (pH 7.2, 0.5 mM EDTA, 150 mM NaCl) at 42 °C. PLL-*g*-Dex and PVS (1.2 times excess) were added successively. (A) N/P=2 (B) N/P=1.2 (C) N/P=1 (D) N/P=0.8 (E) N/P=0.5.

So far, a series of polyelectrolyte-assisted DNA mechanical nanodevices with rapid response were offered, achieving the original aim of this study. As we know, self-complementary stem-loop structures are frequently found in functional DNA and RNA molecules, such as aptamers. Aptamers provide additional functional information about a target protein, which makes them of therapeutic application. Our study in progress is constructing a polyelectrolyte-assisted aptamer-type DNA nanoswitch system that can be instructed repeatedly to bind or release functional proteins, in rapid response to transconformation between the single stem-loop and extended dimer. This nanodivice has potential application as an intelligent drug delivery system.

Conclusions

In summary, a cationic comb-type copolymer, PLL-g-Dex, considerably promoted dimer formation of a self-complementary stem-loop DNA. Dimerization of the stem-loop DNA assisted by PLL-g-Dex was significantly faster than spontaneous dissociation of the dimer. Quick responses were obtained near T_m of the dimer. Stem-loop structures are found naturally in some functional DNA/RNA, such as aptamer. Based on the strategy we have developed here, nanodevices with biological function would permit us to use it in combination with DNA-acting enzymes or other small biomolecules, such as ligase, polymerase, and restrictive proteins. We expect that strategy might extend the applicability of DNA nanodevices in biotechnology and nanotechnology.

Acknowledgements

This work were supported by the National Science Foundation of China (Grant Nos. 21404028, 51362009), "Nanomedicine Molecular Science" (Japan, No. 2306), and Grant-in-Aid for Scientific Research (Japan, No. 23240074). J.D. was supported by the JSPS postdoctoral fellowship. J.C.W. also thanks the Graduate Students Innovation Research Project of Hainan Province.

Notes and references

‡ Electronic supplementary information (ESI) available: Ⅰ Sequences of DIS25, DIS25-2a and DIS25-3a. Ⅱ Structural formula of poly(L-lysine)-graft-dextran (PLL-*g*-Dex). ^{1}H-NMR spectra of PLL-*g*-Dex in D_2O. Ⅲ Gel electrophoretic analysis of dimerization of DIS25 with various N/P ratios. Ⅳ Effect of polyelectrolyte on the fluorescence polarity of TAMRA-labeled duplex. Ⅴ UV absorption/T_m profiles of DIS25. Ⅵ Arrhenius plots for spontaneous dissociation of DIS25 dimer and PLL-*g*-Dex-assisted dimerization of DIS25. Ⅶ Switching between double stem-loop DIS42 and extended multi-plex drived by PLL-g-Dex and PVS.

1 F. A. Aldaye, A. L. Palmer and H. F. Sleiman, *Science,* 2008, **321**, 1795.
2 X. Liu, C. H. Lu and I. Willner, *Acc. Chem. Res.,* 2014, **47**, 1673.
3 A. E. Marras, L. Zhou, H. J. Su and C. E. Castro, *Proc. Natl. Acad. Sci. USA,* 2015, **112**, 713.
4 P. Yin, H. M. Choi, C. R. Calvert and N. A. Pierce, *Nature,* 2008, **451**, 318.
5 T. Goldau, K. Murayama, C. Brieke, S. Steinwand, P. Mondal, M. Biswas, I. Burghardt, J. Wachtveitl, H. Asanuma and A. Heckel, *Chem.-Eur. J.,* 2015, **21**, 2845.
6 Y. Kamiya and H. Asanuma, *Accounts of Chemical Research,* 2014, **47**, 1663.
7 X. Liang, H. Nishioka, N. Takenaka and H. Asanuma, *ChemBioChem,* 2008, **9**, 702.
8 H. Liu, Y. Xu, F. Li, Y. Yang, W. Wang, Y. Song and D. Liu, *Angewandte Chemie International Edition,* 2007, **46**, 2515.
9 Y. Dong, Z. Yang and D. Liu, *Acc. Chem. Res.*, 2014, **47**, 1853.
10 A. Idili, A. Vallée-Bélisle and F. Ricci, *J. Am. Chem. Soc.*, 2014, **136**, 5836.
11 Q. Ke, Y. Zheng, F. Yang, H. Zhang and X. Yang, *Talanta*, 2014, **129**, 539.
12 D. Liu and S. Balasubramanian, *Angew. Chem. Int. Edit.*, 2003, **42**, 5734.
13 S. Modi, M. Swetha, D. Goswami, G. D. Gupta, S. Mayor and Y. Krishnan, *Nat. Nanotechnol.*, 2009, **4**, 325.
14 I. V. Nesterova and E. E. Nesterov, *J. Am. Chem. Soc.*, 2014, **136**, 8843.
15 C. Mao, W. Sun, Z. Shen and N. C. Seeman, *Nature*, 1999, **397**, 144.
16 C. M. Niemeyer, M. Adler, S. Lenhert, S. Gao, H. Fuchs and L. Chi, *ChemBioChem*, 2001, **2**, 260.
17 B. Yurke, A. J. Turberfield, A. P. Mills, F. C. Simmel and J. L. Neumann, *Nature*, 2000, **406**, 605.
18 H. Yan, X. Zhang, Z. Shen and N. C. Seeman, *Nature*, 2002, **415**, 62.
19 W. U. Dittmer, A. Reuter and F. C. Simmel, *Angew. Chem. Int. Edit.*, 2004, **43**, 3550.
20 P. Alberti and J. L. Mergny, *Proc. Natl. Acad. Sci. USA*, 2003, **100**, 1569.
21 Y. Chen, M. Wang and C. Mao, *Angew. Chem. Int. Edit.*, 2004, **43**, 3554.
22 P. Yin, H. Yan, X. G. Daniell, A. J. Turberfield and J. H. Reif, *Angew. Chem. Int. Edit.*, 2004, **43**, 4906.
23 L. Hu, C. H. Lu and I. Willner, *Nano Lett.*, 2015, **15**, 2099.
24 J. Bath and A. J. Turberfield, *Nature Nanotechnol.*, 2007, **2**, 275.
25 P. Alberti, A. Bourdoncle, B. Saccà, L. Lacroix and J. L. Mergny, *Org. Biomol. Chem.*, 2006, **4**, 3383.
26 N. Makita, S. Inoue, T. Akaike and A. Maruyama, *Nucleic Acids Symposium Series*, 2004, **48,** 173.
27 S. W. Choi, N. Makita, S. Inoue, C. Lesoil, A. Yamayoshi, A. Kano, T. Akaike and A. Maruyama, *Nano Lett.*, 2007, **7**, 172.
28 A. Maruyama, M. Katoh, T. Ishihara and T. Akaike, *Bioconjugate Chem.*, 1997, **8**, 3.
29 A. Ferdous, H. Watanabe, T. Akaike and A. Maruyama, *Nucleic Acids Res.*, 1998, **26**, 3949.
30 A. Maruyama, H. Watanabe, A. Ferdous, M. Katoh, T. Ishihara and T. Akaike, *Bioconjugate Chem.*, 1998, **9**, 292.
31 L. Wu, N. Shimada, A. Kano and A. Maruyama, *Soft Matter*, 2008, **4**, 744.
32 W. J. Kim, T. Akaike and A. Maruyama, *J. Am. Chem. Soc.*, 2002, **124**, 12676.
33 W. J. Kim, Y. Sato, T. Akaike and A. Maruyama, *Nat. Mater.*, 2003, **2**, 815.
34 N. Shimada, W. Song and A. Maruyama, *Biomater. Sci.*, 2014, **2**, 1480.
35 K. Yamana, Y. Fukunaga, Y. Ohtani, S. Sato, M. Nakamura, W. J. Kim, T. Akaike and A. Maruyama, *Chem. Commun.*, 2005, 2509.
36 H. Asanuma, T. Osawa, H. Kashida, T. Fujii, X. Liang, K. Niwa, Y. Yoshida, N. Shimada and A. Maruyama, *Chem. Commun.*, 2012, **48**, 1760.
37 J. Michaelis, A. Maruyama and O. Seitz, *Chem. Commun.*, 2013, **49**, 618.
38 K. M. Stewart-Maynard, M. Cruceanu, F. Wang, M.-N. Vo, R. J. Gorelick, M. C. Williams, I. Rouzina and K. Musier-Forsyth, *J. Virol.* 2008, **82**, 10129.
39 G. Krishnamoorthy, B. Roques, J.-L. Darlix and Y. Mély, *Nucleic Acids Res.*, 2003, **31**, 5425.
40 C. Liang, L. Rong, E. Cherry, L. Kleiman, M. Laughrea and M. A. Wainberg, *J. Virol.*, 1999, **73**, 6147.
41 M.-R. Mihailescu and J. P. Marino, *Proc. Natl. Acad. Sci. USA*, 2004, **101**, 1189.